Journal of Molecular Graphics and Modelling 91 (2019) 80–90

Contents lists available at ScienceDirect

Journal of Molecular Graphics and Modelling

journal homepage: www.elsevier.com/locate/JMGM

Erythromycin, Cethromycin and Solithromycin display similar binding affinities to the *E. coli's* ribosome: A molecular simulation study

Hoang Linh Nguyen [a, b], Pham Hong An [a, c], Nguyen Quoc Thai [a, b, d], Huynh Quang Linh [b], Mai Suan Li [e, *]

[a] Institute for Computational Science and Technology, Quang Trung Software City, Tan Chanh, Hiep Ward, District 12, Ho Chi Minh City, Viet Nam
[b] Biomedical Engineering Department, University of Technology – VNU HCM, 268 Ly Thuong Kiet Str., Distr. 10, Ho Chi Minh City, Viet Nam
[c] Department of Theoretical Physics, VNUHCM-University of Science, Ho Chi Minh City, Viet Nam
[d] Dong Thap University, 783 Pham Huu Lau Street, Ward 6, Cao Lanh City, Dong Thap, Viet Nam
[e] Institute of Physics, Polish Acad Sci, Al. Lotnikow 32/46, 02-668, Warsaw, Poland

ARTICLE INFO

Article history:
Received 1 February 2019
Received in revised form
9 May 2019
Accepted 2 June 2019
Available online 4 June 2019

ABSTRACT

Macrolide antibiotics bind to the exit tunnel of the ribosome and inhibit protein synthesis blocking its translocation. Thus, antibiotics including the known macrolide Erythromycin (ERY) are active against bacteria. However, at present, some bacteria show resistance to drugs, which requires the development of new powerful antibacterial agents. One possible way is to use the ERY structure, but change its side chains, while the size of the lactone ring can remain unchanged or change. In this work we consider Cethromycin (CET) and Solithromycin (SOL), which are ketolides with quinolylallyl group at C6 and aminophenyl at C11, respectively (both of them have the same lactone ring as ERY). Experiments have shown that these ketolides have improved efficacy against pathogens, but their binding affinity to the *E. coli*'s ribosome is almost identical. To clarify this issue, we have studied in detail the binding mechanisms of ERY, CET and SOL using the docking and molecular dynamic simulations. In agreement with the experiments, we showed that these compounds have similar binding affinities. Desosamine and lactone ring groups play a critical role in the binding of ERY to the ribosome. In CET and SOL, the contribution of keto and alkylaryl groups is balanced by cyclic carbamate. We have demonstrated that increased fluctuations in the ribosomal residues at the binding site led to an increase in the entropic term in the free binding energy of ERY compared to SOL and CET. The alkyl-aryl arm of both ketolides strongly interacts with A752 and U2609. In addition, the presence of macrolides in the exit tunnel can alter the conformation of U2585, which is located in the peptidyl transferase center, through non-bonded interaction. Therefore, the side chain of ketolides affects not only the binding site but also other residues possibly leading to a strong effect on the protein synthesis process. We predict that to combat bacterial mutations, it is necessary either to design a bulk and charged group as a cladinose, or to use several groups with different signs of charges. This prediction can be used for the development of new efficient antibiotics.

1. Introduction

Macrolides are a class of antibiotics that include a 14–16 membered macrocyclic lactone ring to which one or more sugar groups (usually cladinose and desosamine) can be attached [1]. Macrolides bind to the exit tunnel of the ribosome and might inhibit the synthesis of proteins by blocking its translocation [2]. The first antibiotic of this class, Erythromycin (ERY), exhibits strong activity against a broad range of gram-positive pathogens [3]. ERY is a 14-membered lactone ring macrolide with desosamine and cladinose at C5 and C3 positions of the ring, respectively (Fig. 1). Experiments have shown that the cladinose moiety of ERY plays an important role in ribosome stalling [4]. When bound to the ribosome, the drug contacts with the ribosomal base A2058 through a hydrogen bond between the N1 atom of A2058 and the desosamine hydroxyl [5,6].

Nowadays, some bacteria show resistance to antibiotics, motivating the development of new potent antibacterial agents. One of

* Corresponding author. Institute of Physics, Polish Academy of Sciences, Al. Lotnikow 32/46, 02-668, Warsaw, Poland.
E-mail address: masli@ifpan.edu.pl (M.S. Li).

https://doi.org/10.1016/j.jmgm.2019.06.002
1093-3263/

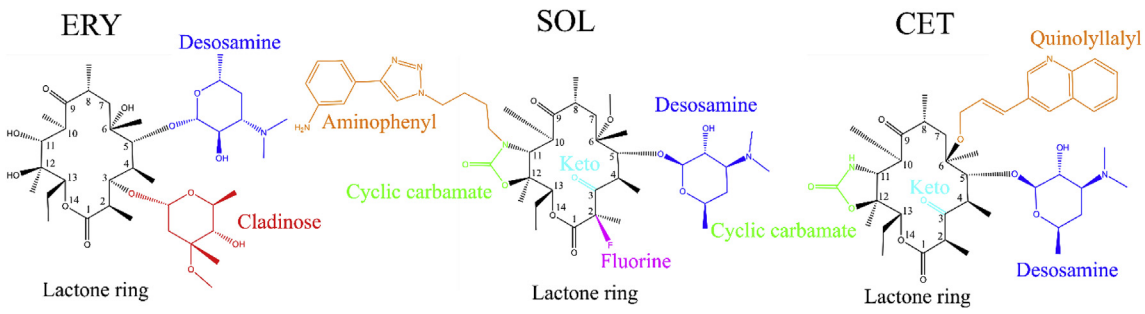

Fig. 1. The chemical structure of Erythromycin, Solithromycin and Cethromycin. Lactone ring and desosamine are common for three compounds. The names of other groups are shown.

the possible strategies is to use the structure of ERY (Fig. 1), but modifying the side chain attached to the lactone ring. This leads to a new generation of macrolides, known as ketolides, which are more effective in antibiotic activity [7,8]. Here the cladinose moiety of macrolides is replaced by keto, and cyclic carbamate and alkyl-aryl group are also present [9] (Fig. 1). Similar to macrolides, ketolides bind to the 50S subunit of the ribosome near A2058 in the exit tunnel inhibiting the elongation of the nascent peptide [6,10]. Experiments revealed that the alkyl chain attached to the carbamate group at position C11-12 interacts with the ribosomal RNA bases A752 and U2609, leading to an increase in the binding affinity of ketolides compared to macrolides [5,11]. Cethromycin (CET) is a ketolide obtained from ERY with a keto group at C3 of the lactone ring and quinolylallyl at position C6, but not at C11 as in the first ketolide Telithromycin. CET exhibits a slightly increased affinity for binding to ribosomes as compared to ERY [12] as well as improved activity against macrolide-resistant pathogens compared to Telithromycin [12]. Due to the specific position of quinolylallyl, the binding mechanism of CET to the ribosome may be different from other ketolides, such as Telithromycin, but this issue has not been solved.

Another new ketolide is Solithromycin (SOL), which is formed by replacing of an alkyl-aryl side chain with 11,12-carbamate-butyl-[1–3]-triazolyl-aminophenyl and a fluorine atom that binds to C2 of the lactone ring (Fig. 1). SOL exhibits a broad spectrum and powerful activity against pathogens [13,14]. Similar to other ketolides, aminophenyl arm at position 11 directly interacts with A752, U2609 [11]. However, these interactions and the presence of a fluorine atom cannot enhance the binding ability of SOL to the ribosome compared to ERY [11]. Llano and coworkers [11] proposed that the contribution of these groups of atoms is counterbalanced by the lack of cladinose, which is present in ERY.

In this work, we explore the interaction of macrolides Erythromycin, Cethromycin and Solithromycin using docking and molecular dynamics simulations. This model study reveals the main factors that govern the binding affinity of macrolides and ketolides to the ribosome. It is also useful for understanding ribosome stalling and bypassing in the presence of antibiotics.

We have shown that, consistent with experimental data [11,15,16], the binding affinities of the three macrolides are slightly different. The desosamine group and the lactone ring make a major contribution to the binding energy of ERY to the ribosome. Unlike ERY, the desosamine group in SOL and CET ketolides weakens the interaction between these ketolides and the ribosome. In the case of SOL, the lack of cladinose is compensated by the aminophenyl and keto groups, whereas the cyclic carbamate group and the fluorine atom significantly reduce the binding affinity due to the repulsive electrostatic interaction. In CET, similarly to SOL, the lactone ring, keto and the alkyl-aryl arm enhance the binding of CET to the ribosome, while the cyclic carbamate has negative impact on the binding. The binding site of CET in the ribosome is similar to Telithromycin and SOL although the quinolylallyl group attaches to C6 of the lactone ring. Moreover, the presence of all studied compounds in the exit tunnel can affect the conformation of base U-2585, which locates in the peptidyl transferase center (PTC).

2. Materials and methods

2.1. Initial structures

The structures of ribosome with ERY and SOL are available in the protein data bank (PDB) with PDB ID 4V7U and 4WWW, respectively. Because the PDB structure of the complex of *E. coli*'s ribosome and CET is not available in PDB, we have obtained it using the docking method. We first removed ERY from 4V7U structure and then this structure was used as a target for docking of CET to the same binding site. To probe the reliability of docking result for CET, we docked ERY and SOL to ribosome structure 4V7U and 4WWW, respectively. Then the obtained binding poses of these drugs were compared to those available in 4V7U and 4WWW holo structures.

2.2. The docking method

AutoDock Tools 1.5.4 [17] was used to prepare the input for docking simulation with PDBQT format. Then, drugs were docked into the receptor by using AutoDock Vina 1.2 [18]. To get reliable results the exhaustiveness was set equal to 400. Ten lowest energy modes of a flexible ligand were generated, while the receptor dynamics was neglected. The difference between the lowest and the highest binding affinity was chosen equal to 7 kcal/mol. The binding site was known from experiment containing residues A2058 and A2059 [5,11,15] and the box was chosen to cover the binding site with grid dimensions $2.3 \times 2.5 \times 2.0$ nm. The lowest binding energy or the energy in the best docking mode was chosen as a scoring function for binding affinity.

2.3. Molecular dynamics (MD) simulation

The MD simulations were performed using GROMACS 2016 package [19]. Parameters of the ribosome structure were obtained from the AMBER99SB-ILDN force field. Antechamber and Acpype were used to calculate force field parameters for small compounds, which are based on the General Amber Force Field (GAFF) [20]. The atomic charges of the compounds were determined using the PROPKA package [21].

The bacterial ribosome consists of two subunits, 30S and 50S (Figure S1). The binding sites of ERY, SOL and CET are located in the

exit tunnel of the ribosome, which is positioned in 50S. Specifically, residues A2058 and A2059 of the binding sites are located in the RNA 23S subunit of 50S.

Because the ribosome is large we have approximated as a sphere of radius of 4 nm, i.e. the residues of ribosome are removed if the distances between them and the center of mass of macrolides are larger than 40 Å. The truncated ribosome consists mainly of the 23S subunit of 50S (Figure S1).

To prevent the spherical truncated ribosome from collapse, but keeping the effect of artificial fixation minimal we followed the procedure proposed by Small et al. [22], where the truncated ribosome was divided into 3 regions. The first region consists of residues that have at least one atom located within 24 Å from center of mass of macrolides. No restraint has been applied to atoms in this region. Residues of the buffer region are located in range between 24 and 32 Å. Atoms in this region are restrained by a harmonic potential with a spring constant 5 kcal/mol/Å^2. Atoms in the rest part of ribosome were restrained by a harmonic potential with a spring constant of 10 kcal/mol/Å^2.

The receptor-drug complexes were solvated in the $12 \times 12 \times 18$ nm box with TIP3P water molecules. Mg^{2+} and Na^{+} ions were added to neutralize the systems, then 0.1M ion Na^{+} and Cl^{-} ions were also added to mimic the salt concentration. A cutoff of 1.0 nm was used to calculate van der Waals (vdW) and electrostatic forces. The particle-mesh Ewald (PME) summation method was employed for calculating the electrostatic energy [23].

First, to remove bad contacts the energy of the system was minimized using the steepest descent algorithm. Then the system was kept at 300K by the v-rescale algorithm in NVT ensemble for 200 ps [24]. The Parrinello-Rahman algorithm was used to run 5 ns NPT equilibration simulation [25]. Finally, each production MD simulation was conducted for 200 ns using the leap-frog integrator. The snapshots sampled at equilibrium were used for data analysis.

The binding free energy of macrolide, ΔG, to the ribosome was calculated by MM-PBSA method [26,27], in which ΔG is given by the following formula:

$$\Delta G = \Delta E_{elec} + \Delta E_{vdW} + \Delta G_{PB} + \Delta G_{sur} - T\Delta S \quad (1)$$

Here ΔE_{elec}, ΔE_{vdW}, ΔG_{PB}, and ΔG_{sur} are electrostatic, van der Waals (vdW) interaction, polar and nonpolar solvation energies, respectively. The electrostatic and vdW interaction energies were calculated without any cutoff using the same parameters that have been used in MD simulations. The polar contribution was calculated by APBS package [28]. The nonpolar term was estimated from the equation $G_{sur} = \gamma * SASA$ with $\gamma = 0.0072$ kcal/mol/Å^2 and SASA is the solvate accessible surface area (Å^2) [29]. The entropy contribution $-T\Delta S$ was obtained using the method proposed by Duan et al. [30]:

$$-T\Delta S = k_B T ln\left\langle e^{\beta E_{rl}^{int}} \right\rangle \quad (2)$$

where $E_{\mathrm{rl}}^{\mathrm{int}}$ is the receptor-ligand interaction energy. In MD simulations the right part of Eq. (2) was calculated as follows

$$\left\langle E^{\beta \Delta E_{rl}^{int}} \right\rangle_{arithmetic} = \frac{1}{N} \sum_{i=1}^{N} e^{\beta E_{rl}^{int}(t_i)} \quad (3)$$

where N is the number of snapshots collected in equilibrium.

A contact between a drug and a base of the ribosome is formed if the distance between center of mass of base and one atom of drug is less or equal 6.5 Å. The experimental binding affinity is calculated from equation $\Delta G\mathrm{exp} = RTln(K_d)$ where the gas constant R = $1.987 * 10^{-3}$ kcal/mol/K, $T = 300$ K and K_{d} is dissociation constant (see, for instance, Borea et al. [31]). RMSD was calculated for heavy atoms of the truncated ribosome and macrolides with respect to the initial structure of MD simulations.

3. Results and discussions

3.1. Docking results

3.1.1. Binding positions

In this work the binding pose corresponds to the conformations obtained in the best docking mode, that is, the conformations with the lowest binding energy. Fig. 2 shows the binding position of ERY, CET and SOL in the ribosome. Although the binding pose of ERY and SOL is known from PDB structures [5,11], we have conducted docking simulation for these drugs in order to verify the accuracy of the docking result obtained for the binding site of CET in *E. coli*'s ribosome.

In the PDB structure 4V7U, ERY is located near residues A2058, A2059 (Fig. 2), and its RMSD relative to the PDB conformation is 0.91 Å. The lactone ring is bound to residues A2058, A2059 but not to A752 and without alkyl-aryl arm, ERY does not form contact with A752 and U2609 bases. This result indicates that our docking position is consistent with the experimental one [5]. In the best docking mode in 4WWW, SOL also binds to residues A-2058 and A2059, while the alkyl-aryl arm is oriented towards A752 and U2609 bases (Fig. 2). The experimental structure 4WWW shows that the alkyl-aryl arm is in contact with the bases A752-U2609 and the lactone ring is associated with A2058-A2059 [11]. The RMSD between this experimental structure and our docking structure is 1.23 Å. Therefore, the configuration of SOL obtained in the docking simulation is similar to the experimental structure [11].

Motivated by the consistency of the ERY and SOL docking poses with the experimental data, we performed a docking simulation for the CET-bound *E. coli*'s ribosome structure 4V7U. In the best docking mode (Fig. 2), the lactone ring is located around A2058 and A2059 bases. The quinolylallyl arm of CET contacts with the A752-U2609 base pair (Fig. 2) and this configuration is similar to the binding pose of Telithromycin [5] and SOL in *E. coli*'s ribosome. However, the C3 keto group of CET is not positioned near U2609 (Fig. 2) as in the D. radiodurans ribosome [32]. This result indicates different orientations of ketolides in the species of bacteria.

Because we will use the structure, obtained in the best docking mode of the CET-ribosome, as the initial conformation for MD simulation and the docking program cannot always gives the correct ranking for different docking poses, we consider the energy and structure of the top 5 best docking modes (Table S1). Obviously, their energy is almost the same and, more importantly, their structures are not different significantly as RMSD with respect to the best docking mode structure remains below 2 Å. This implies that the binding free energy, calculated by MD simulation starting from the structures of top 5 best docking modes, should not depend on the initial configuration. Therefore, in the following, we will present the result, obtained by the MM-PBSA method, using the best docking mode structure as the initial configuration unless otherwise indicated.

3.1.2. Docking binding energy

In the best docking mode, the binding energies of three macrolides are lower than −9.5 kcal/mol (Table 1) suggesting that, in agreement with the with experiment [11,33,34], these drugs strongly bind to the ribosome. In addition, the experimental data indicated that CET and SOL have the binding affinity compatible with ERY [11,15]. Therefore, our binding energies, obtained in the docking simulation, are consistent with experiment.

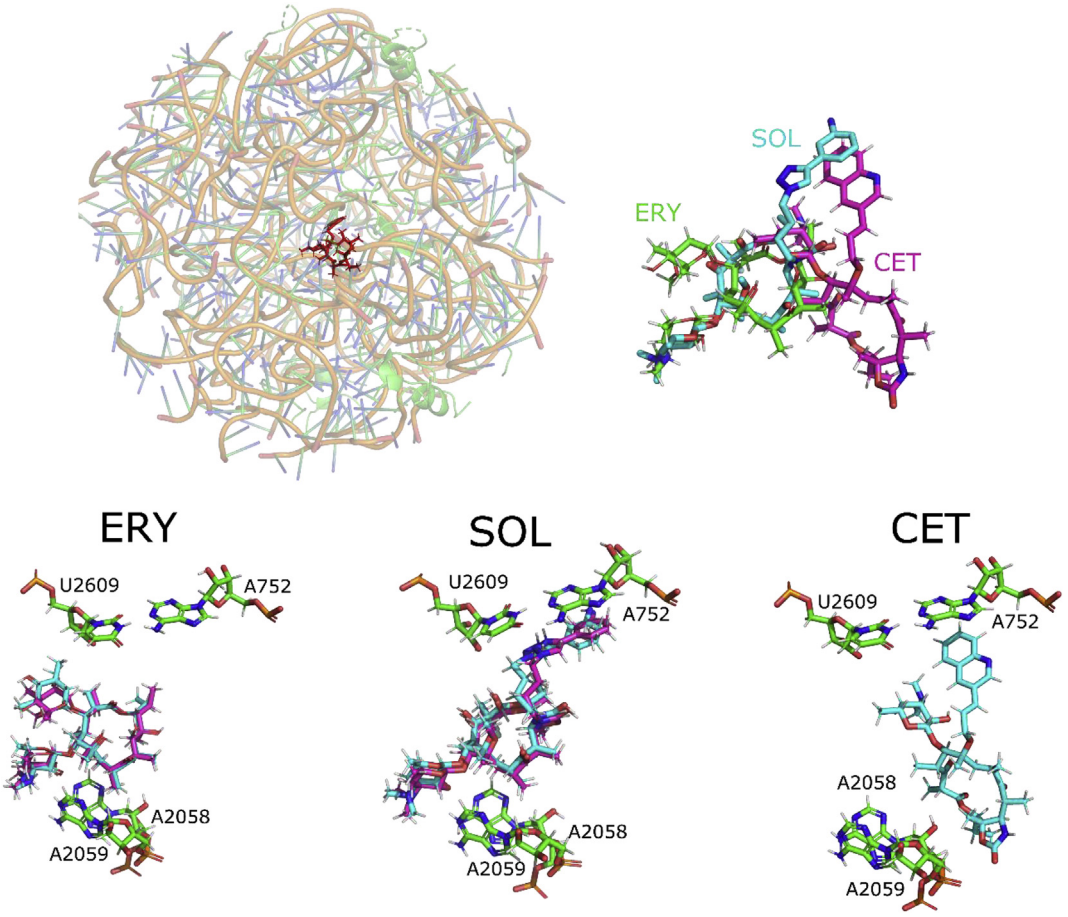

Figure 2. (Upper part - Left) Schematic plot for the initial structure for MD simulations, macrolide is in red. (Upper part - right) The structural alignment in the best docking mode (ribosome is hidden). (Lower part) Locations of the 3 antibiotics in the best docking mode. The structures of ERY and SOL of 4V7U and 4WWW are in magenta, the docking structures are in cyan. *E. coli*'s ribosome structure in ERY and CET cases is 4V7U and 4WWW in SOL case.

Table 1
The docking binding energy and binding free energy ΔG_{bind}, obtained by the MM-PBSA method, for ERY-, CET- and SOL-ribosome complexes. The energy is measured in kcal/mol. Results were averaged over 5 MD trajectories.

	ΔE_{ele}	ΔE_{vdw}	ΔG_{PB}	ΔG_{sur}	$-T\Delta S$	ΔG_{bind}	Docking energy	Experimental ΔG_{bind}
ERY	−224.5	−57.2	260.9	−7.7	13.0	−15.5 ± 1.8	−9.6	−9.9 [11], −10.9 [16]
SOL	−32.8	−71.1	88.1	−9.3	10.4	−14.7 ± 2.2	−11.5	−9.9 [11]
CET	−70.7	−56.5	107.2	−6.6	9.8	−16.8 ± 1.6	−11.1	−12.2 [15]

3.1.3. *Effect of methylation on the binding energy*

It was reported that methylation at the N6 atom group of A2058 base causes resistance of bacteria toward macrolides and ketolides [35–37]. The monomethylation confers high resistance to macrolides but only moderate resistance to ketolides. However, dimethylation causes high resistance to both macrolides and ketolides [36]. To understand these experimental results, we carried out a simulation of the docking of ERY, CET and SOL to the ribosome with the monomethylated and dimethylated N6 atom group of A2058. The chemical structure of methylated A2058 is shown in Figure S2 in SI. The ribosome structure was the same as in the case without methylation. In monomethylation, the binding energy is −6.0, −7.8 and −8.3 kcal/mol for ERY, CET and SOL, respectively (Table S2). Consequently, the binding energy increases by 3.6, 3.3 and 3.2 kcal/mol for ERY, CET and SOL, respectively (compare with Table 1). This result indicates that the effect of monomethylation on ERY stronger than CET and SOL, which is in line with experiments [35–37]. More importantly, in agreement with experiments, monomethylation confers resistance to antibiotics because it impairs the binding affinity (increased binding energy), as shown in our docking result.

In the case of dimethylation, the docking energy is −5.8, −7.5 and −6.8 kcal/mol for ERY, CET and SOL (Table S2), respectively. This result shows that the dimethylation effect is stronger than monomethylation, which is consistent with experiments [35–37]. The increase in the binding energy is 3.8, 3.6 and 4.0 kcal/mol for ERY, CET and SOL, respectively, implying that dimethylation causes high resistance to both macrolides and ketolides, as was observed in the experiment [36].

3.2. *MD results*

3.2.1. *Equilibration procedure*

For MD simulations of ERY- and SOL-ribosome complexes, we used PDB structures 4V7U and 4WWW as the initial conformations. Because a similar PDB structure is not available for the CET-ribosome complex, the best docking pose structure was used as

the initial conformation. To estimate the equilibration time, we have monitored the time dependence of RMSD of the ribosome with respect to its initial conformation. A system is assumed to reach equilibrium if RMSD becomes saturated fluctuating around its equilibrium value. RMSD of the CET-ribosome is higher than in other cases, and, in particular, in three simulations RMSD increases dramatically (Fig. 3). This is due to the fact that, for CET, the simulation started with the best docking structure, whereas for ERY and SOL, the PDB structure, which is better optimized than the docking structure, was used as the initial structure. Simulations with SOL show lower RMSD values (about 0.2–0.4 nm) than RMSD of CET, ERY and empty ribosome. This is probably because the PDB structure of the SOL-ribosome was experimentally resolved better than in other cases.

As evident from Fig. 3, all the studied complexes reached equilibrium after approximately 100 ns. Thus, the snapshots collected at equilibrium, i.e. after 100 ns, were used for computing the binding free energy given by Eq. (1).

3.2.2. ERY, CET and SOL exhibit similar binding affinity to the ribosome

The binding free energy was calculated by Eq. (1). As follows from the time dependence of the interaction entropy [30] (Figure S3), it converges in MD simulations for three complexes. Averaging the final values over five trajectories, we obtained the entropy term shown in Table 1. The differences in the experimental binding free energy of macrolides are insignificant [11,15,16] (Table 1). The binding affinity of CET is slightly higher than ERY and SOL. Using the MM-PBSA method and MD simulation we showed that the binding free energy of CET is lower than that of ERY and SOL (Table 1). However, within error bar the binding affinities of three compounds are almost the same and this result is in good agreement with the experiments. The *in silico* binding affinity of SOL is slightly higher than ERY (Table 1), similar to the experimental data reported by Llano-Sotelo et al. [11].

Although the binding free energy of ERY is compatible with CET and SOL, its electrostatic interaction with the ribosome is significantly lower (Table 1). This is because the charge of ERY is +1 while CET and SOL are neutral. However, the pronounced differences in electrostatic interaction are compensated by the polar term ΔG_{PB}. The van der Waals interaction is strongest in the ribosome-SOL complex, since ΔE_{vdW} is equal to −71.1, −57.2 and −56.5 kcal/mol for SOL, ERY and CET, respectively (Table 1). As expected, the non-polar term ΔG_{sur} is not very sensitive to the compounds under study.

3.2.3. Robustness of the binding affinity against initial structures used for MD simulations

Recall that the results shown in Table 1 were obtained using the PDB structures as the initial structure for MD simulation for the ERY- and SOL-ribosome complexes, whereas for the CET-ribosome it was selected as the best docking mode structure. To study the effect of the initial structure on the binding free energy, we conducted additional MD simulations using the structures obtained in the best docking mode for the ERY- and SOL-ribosomes and the second best docking structure for the CET-ribosome as the initial structures. The setup for these simulations is same as in the previous MD simulations. Within error bar the binding free energy of macrolides (Table S3) remains almost unchanged (compare with Table 1), indicating that the binding affinity is not significantly affected by the initial structures. This is understandable because during the 200 ns MD simulation the ligand has enough time to search for the best position.

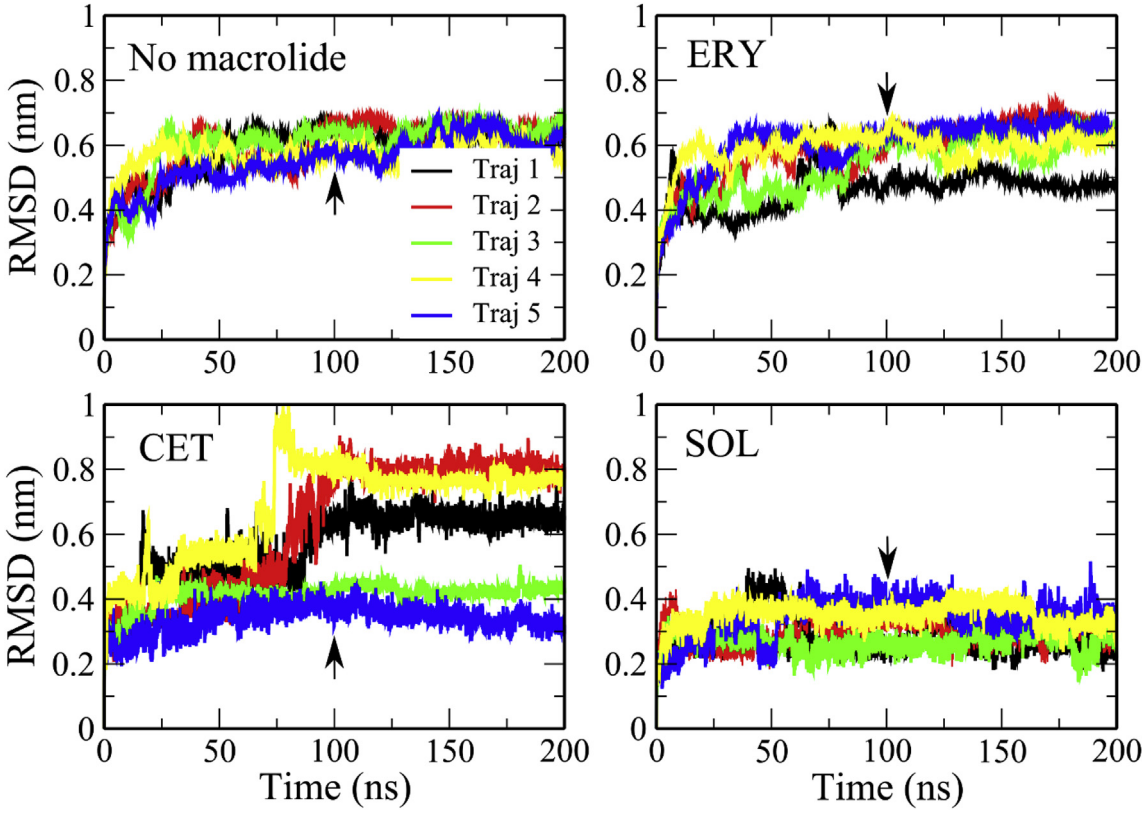

Fig. 3. The time dependence of RMSD of the *E. coli*'s ribosome and ribosome-macrolide complexes (4V7U for apo structure and for holo structures with ERY and CET, and 4WWW for holo structure with SOL). The arrow refers to the time when the complex reaches equilibrium.

3.2.4. Fluctuations of ribosome residues at the binding site contribute to entropy

As can be seen from Table 1, the entropy term of ERY is greater than SOL and CET. To understand this result, we monitor the root mean square fluctuation (RMSF) for macrolide atoms and ribosome residues in the binding site.

Figure S4 shows that the fluctuation of ERY atoms is weaker than SOL and CET and the average RMSF value is 0.06 ± 0.04, 0.10 ± 0.05, and 0.09 ± 0.05 nm for ERY, SOL and CET, respectively. Thus, the average RMSF of ERY is lower than that of SOL and CET by a value of 0.04 and 0.03 nm. This difference is not as significant as in the case of fluctuations of ribosome residues at the binding site, where the average RMSF value is 0.18 ± 0.02, 0.07 ± 0.02 and 0.09 ± 0.03 nm for ERY, SOL and CET respectively (Figure S5). Therefore, we expect that the fluctuation of ribosome residues at the binding site dominates over the fluctuation of macrolide atoms and their strong fluctuations lead to a large entropy of the ribosome-ERY complex.

3.2.5. Contribution of different groups of macrolides to the binding affinity

In order to study in detail the interaction of the macrolide with the ribosome and to identify which component makes the major contribution, we divided the macrolides into blocks (Fig. 1). Lactone ring and desosamine are common for the three compounds. Both CET and SOL have keto and cyclic carbamate groups, but they differ in an additional side chain, in which CET contains quinolylallyl, while aminophenyl belongs to SOL. Atoms of all groups are numbered as shown in Figures S6, S7 and S8 for ERY, CET and SOL, respectively.

In the ERY, the lactone ring exhibits a stronger interaction of vdW with the ribosome compared to the side chain groups desosamine and cladinose (Table 2). Furthermore, it stabilizes the stability of the ribosome-ERY complex by attractive electrostatic interaction having $\Delta E_{elec} = -94.4$ kcal/mol. The cladinose group is dominated by the lactone ring and the desosamine in the electrostatic interaction implying the insignificant role of this side chain group in interaction of ERY and ribosome. Because the cladinose group can interact directly with the nascent chain [38] but not with the ribosome [5], this observation does not contradict the experimental data showing that modification of cladinose significantly affects the ability of the drug to block the protein translocation [4]. The contribution of the desosamine group to the electrostatic interaction is greatest. In general, desosamine and lactone rings, but not cladinose, play a critical role in the binding affinity.

The situation is similar in the case of CET and SOL, where the lactone ring has a significant contribution to electrostatic interaction (Table 2). However, unlike ERY, the desosamine group in these ketolides reduces electrostatic interaction (Table 2). The lactone ring in ERY has the lowest vdW interaction energy while its counterpart in CET has the weakest contribution. The interaction energy between the fluorine atom, attached to C2 of the lactone ring, and the ribosome is 50.7 kcal/mol indicating this atom weakens the binding of SOL to the ribosome. An experimental study revealed that the addition of a fluorine atom to C2 does not significantly affect antibacterial activity [39]. However, Beatriz et al. showed that SOL inhibits the growth of streptococci, which carries the erm gene, more than a drug that does not possess a fluorine atom [11]. The disagreement between these two studies on SOL activity may be due to the fact that the contribution of the fluorine atom to the interaction between SOL and the nascent peptide depends on the sequence of the peptide [40].

Aminophenyl and keto group in SOL have attractive electrostatic interactions with the ribosome (Table 2), but this contribution has been compensated by a cyclic carbamate group, making a total electrostatic interaction weaker than ERY (Table 1). This result is understandable if we take into account the charges of these groups (Table S4-S6, Figure S6-S8). The desosamine and cyclic carbamate groups in CET possess positive electrostatic energy (Table 2) to counteract the attractive electrostatic interaction of the lactone ring, keto and quinolylallyl groups. Thus, the replacement of cladinose by a keto group in CET and SOL radically changes the contribution of the group at C3 of the ring. In addition, the alkyl-aryl side chains in CET and SOL increase the binding of these compounds to the ribosome (Table 2). As for the vdW interaction, the contribution of the lactone ring dominates in all macrolides of CET, SOL and ERY (Table 2). This result can be explained by the fact that the hydrophobic side of these groups binds to A2058, A2059 in the ribosome tunnel (Fig. 2). The common desosamine group stabilizes the complex with ERY, but not with CET and SOL (Table 2).

As evident from Tables 1 and 2, the electrostatic interaction drives the binding of ERY and CET, while the binding strength of SOL is mainly determined by the vdW interaction. The electrostatic interaction is especially important for ERY as this compound is positively charged. The desosamine group and lactone ring control the stability of ERY in complex with the ribosome. In both ketolides, the lactone ring and alkyl-aryl side chains dominate over other side chain groups.

3.2.6. Contact map between macrolides and ribosome

Table 3 shows the top ribosome residues that have the probability of being in contact with ERY, CET and SOL greater than 0.3. Their positions in the ribosome are shown in Fig. 4. The densely populated contact between all drugs and bases A2058 and A2059 is consistent with the experimental and docking results that these residues belong to the binding site [5,11]. In the case of ERY, the ribosomal base A2062 has a high probability of contact, which indicates to its important role in inhibiting protein synthesis. Kannan et al. showed that the mutation A2062U confers resistance to ERY [40], but not ketolide, like telithromycin.

In our work, ketolides SOL and CET have a low probability of contact with A2062 (Table 3) suggesting that A2062 is important only in ERY-dependent ribosome stalling. This result is also

Table 2
Average electrostatic and van der Waals interaction energy (kcal/mol) between atomic groups of macrolide and truncated ribosome. Errors represent standard deviations.

Atom group	ERY		SOL		CET	
	ΔE_{ele}	ΔE_{vdw}	ΔE_{ele}	ΔE_{vdw}	ΔE_{ele}	ΔE_{vdw}
Lactone ring	-94.4 ± 8.4	-33.3 ± 5.8	-129.2 ± 7.4	-30.7 ± 3.8	-104.0 ± 13.0	-22.3 ± 4.1
Desosamine	-152.1 ± 21.0	-11.4 ± 3.0	64.5 ± 13.3	-15.8 ± 1.8	54.7 ± 6.6	-10.8 ± 2.7
Cladinose	22.0 ± 6.0	-12.5 ± 1.2				
Quinolylallyl					-81.1 ± 11.3	-18.3 ± 6.6
Keto			-36.0 ± 2.5	-1.6 ± 0.4	-36.7 ± 8.5	-1.1 ± 0.5
Cyclic carbamate			98.9 ± 8.1	-2.3 ± 0.9	96.4 ± 14.5	-4.0 ± 1.4
Aminophenyl			-81.7 ± 6.9	-23.9 ± 6.3		
Fluorine atom			50.7 ± 1.8	-0.5 ± 0.3		

Table 3
Top residues of the ribosome that have the probability of being in contact with ERY, CET and SOL above or equal 0.3. N/A refers to probabilities that are lower than 0.3. Error represents standard deviation.

Residue	ERY	SOL	CET
U746	N/A	0.8 ± 0.1	1 ± 0.0
A751	N/A	0.7 ± 0.2	0.9 ± 0.3
A752	N/A	1 ± 0.0	0.7 ± 0.2
G2057	0.9 ± 0.2	N/A	N/A
A2058	1 ± 0.0	1 ± 0.0	1 ± 0.0
A2059	1 ± 0.0	1 ± 0.0	0.8 ± 0.3
A2062	0.6 ± 0.3	0.3 ± 0.2	N/A
A2503	0.7 ± 0.2	0.8 ± 0.2	N/A
U2609	0.4 ± 0.3	0.8 ± 0.2	0.5 ± 0.1
C2610	1 ± 0.0	0.9 ± 0.1	0.3 ± 0.1
C2611	1 ± 0.0	1 ± 0.0	0.6 ± 0.1

consistent with the weak effect of SOL and CET on the torsion angle of A2062, while ERY has a much stronger effect (see below). The bases C2610 and A2503 are sensors of the drug structure [4], which have different probabilities of contact with ERY, SOL and CET. Indeed, while ERY and SOL have a high contact population with C2610 and A2503 (Table 3), CET occasionally makes contact with these bases. This reflects the distinctive characteristics of the quinolylallyl group attached to C6 of the ring of CET.

Both ketolides SOL and CET have strong contact with U746, A751, A752 and U2609 (Table 3), while ERY only strongly interacts with U2609. Similar behavior was also observed for Telithromycin [5]. Dunkle et al. showed that Telithromycin can protect A752 from a chemical probe due to the interaction between the alkyl-aryl arm and the A752-U2609 pair [5]. Our result shows that, like Telithromycin, SOL and CET have close contact with the pair A752-U2609, which can play an important role in resistance to these drugs. The interaction between CET and A752 in *E. coli* is different from D. radiodurans [32], in which CET interacts only with U2609 because D. radiodurans does not have U2609-A752 pair. Although the quinolylallyl group attached to C6 in the lactone ring, this group also has the same interaction network as the alkyl-aryl moiety that is attached to C11 in other ketolides.

3.2.7. Hydrogen bonds between macrolides and ribosome

First, we consider a hydrogen bond (HB) network of the structures used as initial conformations for MD simulations (Figure S9). For ERY- and SOL-ribosome complexes, they are 4V7U and 4WWW PDB structures, respectively. In the case of CET-ribosome, we have the best docking pose when CET is bound to the 4V7U PDB structure. Obviously, ERY does not form HB with the ribosome, while SOL and CET forms one HB with A2059 (Figure S9).

We calculated the average number of HBs between the atom groups of ERY, SOL and CET and the ribosome during MD simulation at equilibrium (Table 4). ERY forms HB only with the lactone ring and the mean value of HBs is low (0.4 ± 0.2). In the SOL case, the lactone ring does not have HB (Table 4), but desosamine forms HB with an average value of 0.4 ± 0.2. Cyclic carbamate occasionally has hydrogen bonding with the ribosome (0.2 ± 0.1), while aminophenyl forms HB during the entire MD simulation at equilibrium (0.9 ± 0.2). For CET, all atom groups form HB but their population is low (Table 4). The number of HBs between the ribosome and the cyclic carbamate group in CET and SOL is the same. However, the keto group in CET has a higher propensity to hydrogen bonding than in SOL.

Base A2058 of the ribosome forms HB with all macrolides (Table S7). CET and SOL also form HB with bases A751 and A752, while ERY does not have HB with these bases. U746 forms HB only with SOL.

As follows from Table 4 and S7, the hydrogen bonding between macrolides and the ribosome is weak, implying that it is not a main factor that controls the stability of the macrolide-ribosome complexes.

3.2.8. The interaction energy of the most important residues with macrolides

In this section we consider the non-bonded interaction of macrolides with residues whose contact probability exceeds 0.3 (Table 3). All macrolides strongly interact with A2058 and A2059

Table 4
Average number of hydrogen bonds between macrolides and ribosome. Results were averaged over 5 MD trajectories. Error represents standard deviation.

Atom group	ERY	SOL	CET
Lactone ring	0.4 ± 0.2	N/A	0.4 ± 0.1
Desosamine	0.0 ± 0.0	0.4 ± 0.2	0.2 ± 0.1
Cladinose	0.0 ± 0.0		
Quinolylallyl			0.2 ± 0.1
Keto		0.0 ± 0.0	0.3 ± 0.1
Cyclic carbamate		0.2 ± 0.1	0.3 ± 0.1
Aminophenyl		0.9 ± 0.2	
Fluorine atom		0.0 ± 0.0	

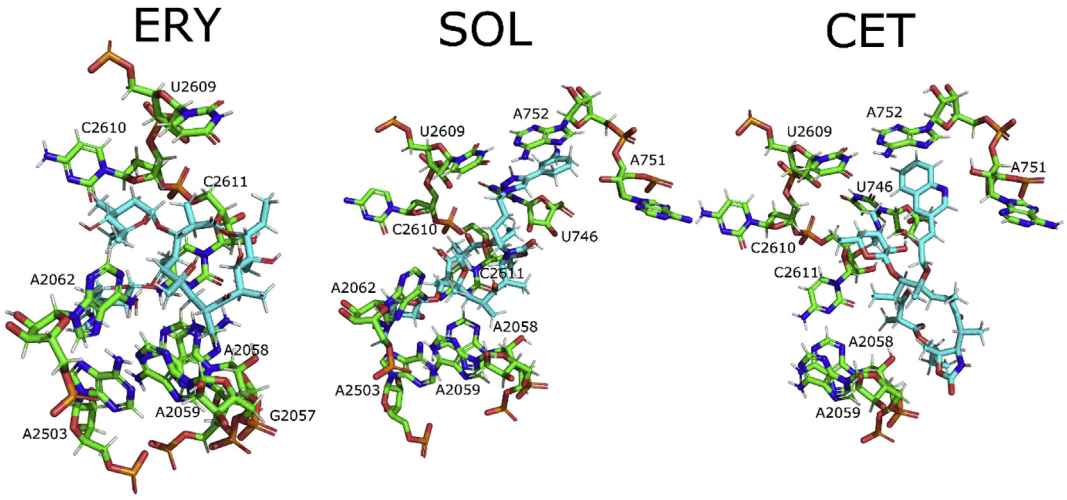

Fig. 4. Macrolides (cyan) and residues that have a probability of contact with the macrolide more than 0.3.

(Table 5) as are located in the binding site. In accordance with the total interaction energy (Table 1), ERY has the strongest electrostatic energy. The high attractive interaction of residue A2062 with ERY is consistent with the fact that the presence of ERY alters the conformation of A2062. Both CET and SOL interact with U746, A751, and A752-U2609, but the interaction of these residues with CET is stronger than with SOL (Table 5), showing different characteristics of alkyl-aryl arms during the interaction of these ketolides and ribosome residues. This is also in the line with the results obtained for the total interaction energy (Table 2).

3.2.9. *Effect of macrolides on the configuration of specific bases of the ribosome*

To study the effect of three drugs on the conformations of specific ribosomal bases, we calculated the distributions of their torsion angles (Fig. 5). When no drug is bound to the ribosome, the distribution has one and two peaks for bases A2058 and A2059 at the binding site, respectively. However, in the presence of macrolides, the peak of the distribution of A2058 torsion angle shifts (Fig. 5). For A2059, ERY maintains a two-peak structure, while one peak is observed in the presence of CET and SOL. Thus, the conformations of A2058 and A2059 bases are reordered to accommodate the macrolide at the binding site. This result is consistent with experiments showing that macrolides directly interact with these bases [5,11].

Because the position of the A2062 residue is close to macrolides in the exit tunnel, it can narrow or expand the tunnel space by reorientation. The torsion angle of A2062 changed dramatically in the presence of ERY and CET (Fig. 5), which changes the size of the tunnel. When these drugs are bound, one peak is divided into 2 separate peaks. However, it altered only slightly in the presence of SOL indicating a variety of macrolide effects on the A2062 configuration. Our observations agree with an experiment on the role of mutations at this residue in ERY dependent ribosome stalling [41].

Because the bases A2503, U2609 and C2610 are located next to the macrolide, their torsion angles are sensitive to the macrolide types (Fig. 5). The distribution of the A2503 torsion angle changes dramatically when macrolide binds. Only SOL preserves a single-peak structure, but the peak position is offset. All three compounds significantly change the torsion angle of U2609 and C2610. On the other hand, experiments have shown that bases A2503, U2609 and C2610 regulate the structure of the drug, and therefore mutations at these positions can change the drug activity [4,15,42]. Our results, at least in part, confirm this experimental fact.

Although macrolides bind to the exit tunnel at residues A2058, A2059, but not to the peptidyl transferase center (PTC) they can effect residue U2585, which is located in PTC. In the presence of all three macrolides, the configuration of U2585 varies greatly, because instead of one pronounced peak, we obtained two peaks in the distribution of its dihedral angle (Fig. 5). This result is consistent with Sothiselvam et al. [43], who reported that ERY contributes to the reorientation of U2585. Therefore, the presence of macrolides can cause a conformation change in PTC and, consequently, change the protein translation.

In the presence of CET and SOL, the distribution of the torsion angle of A-752 varies not only in the number of peaks, but also in their position (Fig. 5). This is consistent with the docking and experimental data collected for SOL, in which the alkyl-aryl moiety is in contact with A752 [11]. In the case of ERY, the distribution has two peaks, but they are shifted (Fig. 5).

3.2.10. *Molecular mechanism for changing the conformation of U2585 in the presence of a macrolide*

Based on the simulation results, Sothiselvam et al. proposed two ways in which, in the absence of an emerging peptide, ERY could change the orientation of U2585, rotating the bases connecting the drug and U2585 [44]. In the first way, the first step is the A2062 rotation, which causes a change in the conformation of its neighbors G2061 and C2063, while the second path is initiated by reorienting U2609 then the second step of this path is communication with PTC through U1782 and U2586 (Fig. 6). Thus, macrolides can indirectly change the conformation of U2585.

In the case of ERY, the orientation of the dihedral angle of A2062 is changed supporting the pathway starting from A2062. However, the effect of ERY on the dihedral angle of C2063 is insignificant (Figure S10). SOL has a slight effect on the torsion angle of A2062 (Fig. 5) as well as the A2062-SOL contact is poorly populated, while the influence of SOL on G2061 and G2063 is strong (Figure S10). Thus, it is unlikely that the pathway starting from A2062 is responsible for the reorientation of U2585 in the presence of macrolides. Changes in dihedral angles of bases A2062, G2061 and C2063 are independent each other, or in other words, there is no coherent rotation of these bases, when macrolides are bound to the ribosome.

Although all studied macrolides modulate dramatically the dihedral angle of U2609 (Fig. 5), the conformation of its neighbors U1782, U2586 remain almost unchanged (Figure S11). This result indicates that the presence of macrolides do not cause a reorientation of U2585 by the second pathway starting from U2609. Thus, the two paths proposed by Sothiselvam et al. [44] were not supported by our simulation. Instead, we assume that the presence of macrolides alters the conformation of U2585 through a non-bonded interaction between PTC and neighboring bases. The non-bonded interaction energy between U-2585 and ERY, CET and SOL is −2.3, −1.3, −1.2 kcal/mol, respectively. Since U2585 does not form contact with another nucleotides like A752-U2609 pair, a

Table 5
Interaction energy (kcal/mol) between macrolides and the most important ribosome residues (see Table 3). N/As refer to energies that are not calculated. Error represents standard deviation.

	ERY		SOL		CET	
	ΔE_{ele}	ΔE_{vdw}	ΔE_{ele}	ΔE_{vdw}	ΔE_{ele}	ΔE_{vdw}
U746	N/A	N/A	4.4 ± 1.0	−6.9 ± 1.0	1.0 ± 1.3	−2.7 ± 0.8
A751	N/A	N/A	2.1 ± 0.6	−3.3 ± 0.7	−1.7 ± 0.9	−8.0 ± 1.8
A752	N/A	N/A	1.7 ± 1.0	−8.5 ± 1.8	2.6 ± 1.5	−9.2 ± 1.7
G2057	−8.9 ± 1.5	−1.4 ± 0.3	N/A	N/A	N/A	N/A
A2058	−9.0 ± 2.1	−7.1 ± 0.8	−8.4 ± 1.7	−7.8 ± 1.2	−3.1 ± 1.2	−2.8 ± 0.9
A2059	−6.3 ± 2.3	−6.2 ± 1.7	−3.4 ± 0.9	−6.2 ± 1.4	−4.7 ± 1.0	−3.3 ± 0.8
A2062	−6.3 ± 2.1	−2.6 ± 1.0	−2.3 ± 0.4	−2.0 ± 1.0	N/A	N/A
A2503	−8.8 ± 2.2	−2.8 ± 1.2	−3.0 ± 0.8	−4.1 ± 1.3	N/A	N/A
U2609	−5.0 ± 0.9	−2.6 ± 1.2	2.6 ± 1.1	−4.6 ± 1.4	−2.4 ± 0.8	−4.6 ± 1.2
C2610	−8.3 ± 1.5	−6.0 ± 0.8	1.1 ± 0.4	−5.3 ± 1.4	−1.5 ± 1.0	−2.1 ± 1.2
C2611	−7.6 ± 2.4	−12.1 ± 0.5	−1.5 ± 1.1	−9.5 ± 1.4	−2.2 ± 1.3	−4.2 ± 1.4

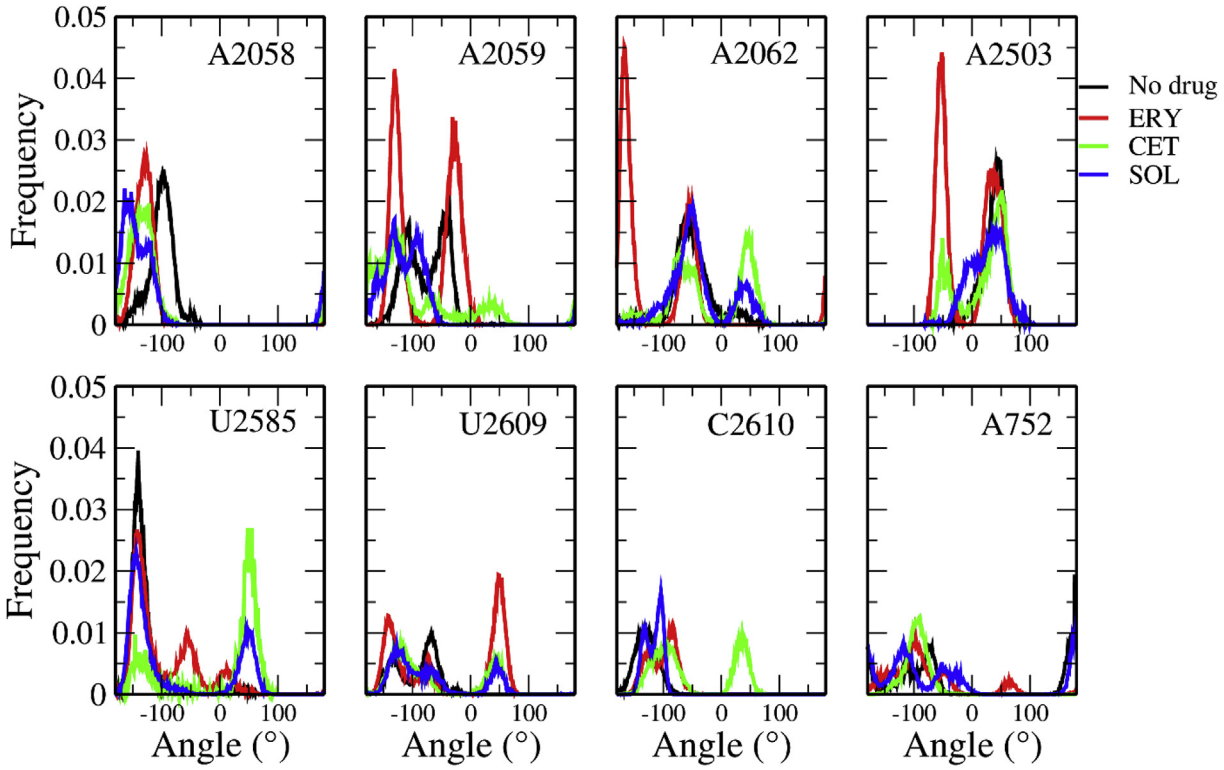

Fig. 5. Distributions of torsion angles for specific ribosomal bases.

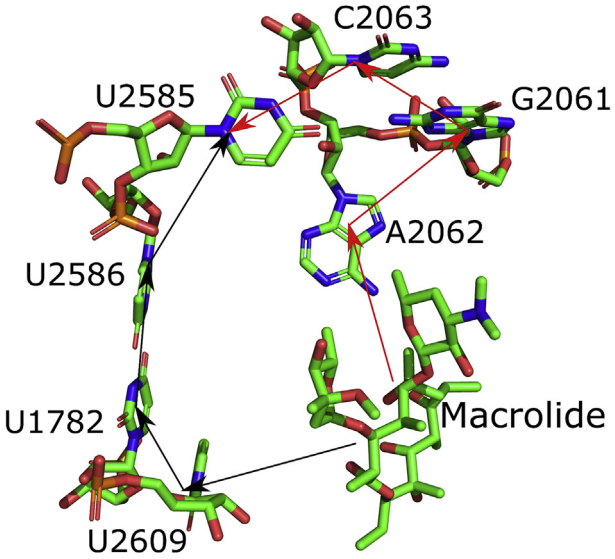

Fig. 6. Two possible paths through which macrolide can indirectly change the conformation of U2585 located in PCT. The first pathway that begins with A-2062 is described by red arrows. The second pathway, indicated by black arrow, starts with U2609. (For interpretation of the references to colour in this figure legend, the reader is referred to the Web version of this article.)

small change in this interaction energy may be sufficient to change its torsion angle. Moreover, the rotation of neighboring U2585 bases can cause fluctuations in the interaction between them and U2585, which augments the effect of macrolides on the conformation of U2585. This mechanism is supported by experimental evidence that mutations at A2062, U2609, U2586, and U1782, which are involved in both pathways, exert only a minor effect on ERY-dependent stalling of MRL peptide [44].

4. Discussion and conclusions

We have shown that the lactone ring and desosamine groups dominate in the interaction between ERY and the ribosome. The keto group and alkyl-aryl arm in SOL counterbalance cyclic carbamate and desosamine groups in both ketolides. This may explain the broad spectrum of activity against the pathogens of these ketolides, since the contribution of their side chain groups is more diverse than in ERY. The role of the lactone ring is to enhance the binding of ERY, SOL and CET to the ribosome (Table 2). The opposite has happened to desosamine, as shown in Table 2, it increases the binding affinity in the case of ERY, but reduces the interaction between ketolides and the ribosome. We found that increased fluctuations of the ribosomal residues at the binding site led to an increase in the entropic term in the free binding energy of ERY compared to SOL and CET.

From docking and MD simulations, we learned that the CET binding site in the *E. coli* ribosome is similar to other ketolides. The alkyl-aryl chain in CET and SOL causes the corresponding ketolides to come into contact with A752-U2609, whereas such a contact does not exist in the ERY case. Furthermore, the alkyl-aryl arms in CET and SOL increase the interaction energy between these ketolides and ribosome residues.

We have studied the effect of methylation in the N6 atom group of the A2058 base on the binding affinity of antibiotics using the docking method. It was demonstrated that both monomethylation and dimethylation reduce the absolute value of the binding energy and this result is consistent with experiments, which showed that methylation confers resistance of bacteria to macrolides and ketolides. It would be interesting to conduct an all-atom MD simulation in order to gain a deeper understanding of the molecular mechanism of binding with methylation.

It is known that some nascent peptides can be stalled only when interacting with a specific drug [38,40,45]. Although the binding affinity of ketolides CET and SOL is similar to ERY, they are superior to ERY in antibiotic activity [12,13]. Alkyl-aryl arms and keto groups in CET and SOL enhance their interaction with the ribosome, but the binding affinity of these ketolides is slightly different from ERY because of the presence of cyclic carbamate group. However, the difference in the sign of their charges (Table S7 and S8) can lead to an advantage in inhibiting the translocation of the nascent peptides. More precisely, ERY has only three groups in which the cladinose has a negative charge, while others have a positive charge. CET and SOL have even more groups with different positive and negative charges. This characteristic of CET and SOL can contribute more to their resistance to mutations compared to ERY, since the residues of the nascent peptide can experience attractive interaction with one of the groups, as evidenced by the fact that ketolides are effective against macrolide-resistant strains [1,46]. However, the presence of groups with different charge signs can balance each other and weaken the interaction between ketolides and peptides, making it easier for nascent peptides to bypass ketolides. For example, the first ketolide Telithromycin is bypassed more often than ERY [40,47]. Therefore, we predict that to fight bacterial mutations, one must either to create a bulk and charged group as cladinose, or use several groups with charges of different signs. This prediction may be useful for designing new potent antibiotics.

Finally, we have shown that the interaction of ERY and ribosome differs from SOL and CET both in binding sites and in the interaction energy of different groups. Our previous study demonstrated that ERY affects the translocation of ErmCL and H-NS through non-bonded interaction with these peptides [48]. From this point of view, the nature of the ribosome stalling caused by SOL and CET may be different from ERY. This intriguing problem must be solved in the future work.

Author contributions

MSL conceived the experiment. HLN, PHA and NQT conducted the experiment. HLN, PHA, NQT and MSL analyzed the results. MSL and HLN wrote the paper. All authors reviewed the manuscript.

Funding sources

This work was supported by Department of Science and Technology at Ho Chi Minh city, Vietnam, and the Polish NCN grant 2015/19/B/ST4/02721, Poland. This research was also funded by Ho Chi Minh City University of Technology, VNU-HCM, under grant number BK-SDH-2019-1880315.

Notes

The authors declare no competing financial interest.

Appendix A. Supplementary data

Supplementary data to this article can be found online at https://doi.org/10.1016/j.jmgm.2019.06.002.

References

[1] P. Fernandes, E. Martens, D. Pereira, Nature nurtures the design of new semi-synthetic macrolide antibiotics, J. Antibiot. 70 (2017) 527.
[2] M. Gaynor, A.S. Mankin, Macrolide antibiotics: binding site, mechanism of action, resistance, Curr. Top. Med. Chem. 3 (2003) 949–960.
[3] N.L. Oleinick, The erythromycins, in: Mechanism of Action of Antimicrobial and Antitumor Agents, Springer, 1975, pp. 396–419.
[4] N. Vázquez-Laslop, D. Klepacki, D.C. Mulhearn, H. Ramu, O. Krasnykh, S. Franzblau, et al., Role of antibiotic ligand in nascent peptide-dependent ribosome stalling, Proc. Natl. Acad. Sci. U. S. A. 108 (2011) 10496–10501.
[5] J.A. Dunkle, L. Xiong, A.S. Mankin, J.H. Cate, Structures of the Escherichia coli ribosome with antibiotics bound near the peptidyl transferase center explain spectra of drug action, Proc. Natl. Acad. Sci. U. S. A. 107 (2010) 17152–17157.
[6] L.H. Hansen, P. Mauvais, S. Douthwaite, The macrolide–ketolide antibiotic binding site is formed by structures in domains II and V of 23S ribosomal RNA, Mol. Microbiol. 31 (1999) 623–631.
[7] J. Andrews, T. Weller, J. Ashby, R. Walker, R. Wise, The in vitro activity of ABT773, a new ketolide antimicrobial agent, J. Antimicrob. Chemother. 46 (2000) 1017–1022.
[8] G. Ackermann, A.C. Rodloff, Drugs of the 21st century: telithromycin (HMR 3647)—the first ketolide, J. Antimicrob. Chemother. 51 (2003) 497–511.
[9] G.G. Zhanel, M. Dueck, D.J. Hoban, L.M. Vercaigne, J.M. Embil, A.S. Gin, et al., Review of macrolides and ketolides, Drugs 61 (2001) 443–498.
[10] W.S. Champney, C.L. Tober, Structure–activity relationships for six ketolide antibiotics, Curr. Microbiol. 42 (2001) 203–210.
[11] B. Llano-Sotelo, J. Dunkle, D. Klepacki, W. Zhang, P. Fernandes, J.H. Cate, et al., Binding and action of CEM-101, a new fluoroketolide antibiotic that inhibits protein synthesis, Antimicrob. Agents Chemother. 54 (2010) 4961–4970.
[12] V.D. Shortridge, P. Zhong, Z. Cao, J.M. Beyer, L.S. Almer, N.C. Ramer, et al., Comparison of in vitro activities of ABT-773 and telithromycin against macrolide-susceptible and-resistant streptococci and staphylococci, Antimicrob. Agents Chemother. 46 (2002) 783–786.
[13] S.D. Putnam, H.S. Sader, D.J. Farrell, D.J. Biedenbach, M. Castanheira, Antimicrobial characterisation of solithromycin (CEM-101), a novel fluoroketolide: activity against staphylococci and enterococci, Int. J. Antimicrob. Agents 37 (2011) 39–45.
[14] J. Mallegol, P. Fernandes, R.G. Melano, C. Guyard, Antimicrobial activity of solithromycin against clinical isolates of Legionella pneumophila serogroup 1, Antimicrob. Agents Chemother. 58 (2014) 909–915.
[15] G. Garza-Ramos, L. Xiong, P. Zhong, A. Mankin, Binding site of macrolide antibiotics on the ribosome: new resistance mutation identifies a specific interaction of ketolides with rRNA, J. Bacteriol. 183 (2001) 6898–6907.
[16] S. Pestka, Binding of [14C] erythromycin to Escherichia coli ribosomes, Antimicrob. Agents Chemother. 6 (1974) 474–478.
[17] M.F. Sanner, Python: a programming language for software integration and development, J. Mol. Graph. Model. 17 (1999) 57–61.
[18] O. Trott, A.J. Olson, AutoDock Vina: improving the speed and accuracy of docking with a new scoring function, efficient optimization, and multithreading, J. Comput. Chem. 31 (2010) 455–461.
[19] M.J. Abraham, T. Murtola, R. Schulz, S. Páll, J.C. Smith, B. Hess, et al., GROMACS: high performance molecular simulations through multi-level parallelism from laptops to supercomputers, SoftwareX 1 (2015) 19–25.
[20] J. Wang, R.M. Wolf, J.W. Caldwell, P.A. Kollman, D.A. Case, Development and testing of a general amber force field, J. Comput. Chem. 25 (2004) 1157–1174.
[21] M.H. Olsson, C.R. Søndergaard, M. Rostkowski, J.H. Jensen, PROPKA3: consistent treatment of internal and surface residues in empirical p K a predictions, J. Chem. Theory Comput. 7 (2011) 525–537.
[22] M.C. Small, P. Lopes, R.B. Andrade, A.D. MacKerell Jr., Impact of ribosomal modification on the binding of the antibiotic telithromycin using a combined grand canonical Monte Carlo/molecular dynamics simulation approach, PLoS Comput. Biol. 9 (2013), e1003113.
[23] T. Darden, D. York, L. Pedersen, Particle mesh Ewald: an N· log (N) method for Ewald sums in large systems, J. Chem. Phys. 98 (1993) 10089–10092.
[24] G. Bussi, D. Donadio, M. Parrinello, Canonical sampling through velocity rescaling, J. Chem. Phys. 126 (2007), 014101.
[25] M. Parrinello, A. Rahman, Polymorphic transitions in single crystals: a new molecular dynamics method, J. Appl. Phys. 52 (1981) 7182–7190.
[26] J. Srinivasan, J. Miller, P.A. Kollman, D.A. Case, Continuum solvent studies of the stability of RNA hairpin loops and helices, J. Biomol. Struct. Dyn. 16 (1998) 671–682.
[27] P.A. Kollman, I. Massova, C. Reyes, B. Kuhn, S. Huo, L. Chong, et al., Calculating structures and free energies of complex molecules: combining molecular mechanics and continuum models, Acc. Chem. Res. 33 (2000) 889–897.
[28] E. Jurrus, D. Engel, K. Star, K. Monson, J. Brandi, L.E. Felberg, et al., Improvements to the APBS biomolecular solvation software suite, Protein Sci. 27 (2018) 112–128.
[29] W.C. Still, A. Tempczyk, R.C. Hawley, T. Hendrickson, Semianalytical treatment of solvation for molecular mechanics and dynamics, J. Am. Chem. Soc. 112 (1990) 6127–6129.
[30] L. Duan, X. Liu, J.Z. Zhang, Interaction entropy: a new paradigm for highly efficient and reliable computation of protein–ligand binding free energy, J. Am. Chem. Soc. 138 (2016) 5722–5728.
[31] P.A. Borea, K. Varani, S. Gessi, P. Gilli, A. Dalpiaz, in: Receptor Binding Thermodynamics as a Tool for Linking Drug Efficacy and affinity1Presented at the First Italian–Swiss Meeting on Medicinal Chemistry, Turin, Italy, September 1997.1. Farmaco, vol 53, 1998, pp. 249–254.
[32] F. Schlünzen, J.M. Harms, F. Franceschi, H.A. Hansen, H. Bartels, R. Zarivach, et al., Structural basis for the antibiotic activity of ketolides and azalides, Structure 11 (2003) 329–338.
[33] Z. Cao, P. Zhong, X. Ruan, P. Merta, J.O. Capobianco, R.K. Flamm, et al., Ribosome affinity and the prolonged molecular postantibiotic effect of cethromycin (ABT-773) in Haemophilus influenzae, Int. J. Antimicrob. Agents 24 (2004) 362–368.

[34] G.-R. Georgina, L. Xiong, P. Zhong, A. Mankin, Binding site of macrolide antibiotics on the ribosome: new resistance mutation identifies a specific interaction of ketolides with rRNA, J. Bacteriol. 183 (2001) 6898–6907.
[35] B. Vester, L.H. Hansen, S.J.R. Douthwaite, The Conformation of 23S rRNA Nucleotide A2058 Determines its Recognition by the ErmE Methyltransferase, vol. 1, 1995, pp. 501–509.
[36] M.M. Almutairi, S.R. Park, S. Rose, D.A. Hansen, N. Vázquez-Laslop, S. Douthwaite, et al., Resistance to Ketolide Antibiotics by Coordinated Expression of rRNA Methyltransferases in a Bacterial Producer of Natural Ketolides, vol 112, 2015, pp. 12956–12961.
[37] M. Liu, S.J.A.A. Douthwaite, Chemotherapy. Activity of the Ketolide Telithromycin is Refractory to Erm Monomethylation of Bacterial rRNA, vol 46, 2002, pp. 1629–1633.
[38] S. Arenz, S. Meydan, A.L. Starosta, O. Berninghausen, R. Beckmann, N. Vázquez-Laslop, et al., Drug Sensing by the ribosome induces translational arrest via active site perturbation, Mol. Cell 56 (2014) 446–452.
[39] R.F. Keyes, J.J. Carter, E.E. Englund, M.M. Daly, G.G. Stone, A.M. Nilius, et al., Synthesis and antibacterial activity of 6-O-arylbutynyl ketolides with improved activity against some key erythromycin-resistant pathogens, J. Med. Chem. 46 (2003) 1795–1798.
[40] K. Kannan, N. Va'zquez-Laslop, A.S. Mankin, Selective protein synthesis by ribosomes with a drug-obstructed exit tunnel, Cell 151 (2012) 508–520.
[41] N. Vazquez-Laslop, C. Thum, A.S. Mankin, Molecular mechanism of drug-dependent ribosome stalling, Mol. Cell 30 (2008) 190–202.
[42] N. Vázquez-Laslop, H. Ramu, D. Klepacki, K. Kannan, A.S. Mankin, The key function of a conserved and modified rRNA residue in the ribosomal response to the nascent peptide, EMBO J. 29 (2010) 3108–3117.
[43] S. Sothiselvam, B. Liu, W. Han, H. Ramu, D. Klepacki, G.C. Atkinson, et al., Macrolide antibiotics allosterically predispose the ribosome for translation arrest, Proc. Natl. Acad. Sci. U. S. A. 111 (2014) 9804–9809.
[44] S. Sothiselvam, B. Liu, W. Han, H. Ramu, D. Klepacki, G.C. Atkinson, et al., Macrolide antibiotics allosterically predispose the ribosome for translation arrest, Proc. Natl. Acad. Sci. U. S. A. 111 (2014) 9804–9809.
[45] P. Gupta, B. Liu, D. Klepacki, V. Gupta, K. Schulten, A.S. Mankin, et al., Nascent peptide assists the ribosome in recognizing chemically distinct small molecules, Nat. Chem. Biol. 12 (2016) 153.
[46] A. Bonnefoy, A. Girard, C. Agouridas, J. Chantot, Ketolides lack inducibility properties of MLS (B) resistance phenotype, J. Antimicrob. Chemother. 40 (1997) 85–90.
[47] K. Kannan, P. Kanabar, D. Schryer, T. Florin, E. Oh, N. Bahroos, et al., The general mode of translation inhibition by macrolide antibiotics, Proc. Natl. Acad. Sci. U. S. A. 111 (2014) 15958–15963.
[48] H.L. Nguyen, D.L. Pham, E.P. O'Brien, M.S. Li, Erythromycin leads to differential protein expression through differences in electrostatic and dispersion interactions with nascent proteins, Sci. Rep. 8 (2018) 1–11.